

DYNAMIC TESTING OF A SUBSCALE SUNSHIELD FOR THE NEXT GENERATION SPACE TELESCOPE (NGST)

Brian P. Ross, John D. Johnston, and James T. Smith

NASA Goddard Space Flight Center

ABSTRACT

The NGST sunshield is a lightweight, flexible structure consisting of pretensioned membranes supported by deployable booms. The structural dynamic behavior of the sunshield must be well understood in order to predict its influence on observatory dynamic performance. A 1/10th scale model of the sunshield has been developed for ground testing to provide data to validate modeling techniques for thin-film membrane structures. The validated models can then be used to predict the behavior of the full-scale sunshield. This paper provides an overview of two test series performed on the 1/10th scale sunshield and a comparison of the results from the tests.

INTRODUCTION

The Next Generation Space Telescope (NGST) requires a large sunshield to passively cool the telescope and detectors. A conceptual design for the NGST observatory, referred to as the 'yardstick' concept, was developed by NASA to establish a reference design for the mission and identify areas in need of technology development. The 'yardstick' concept sunshield consists of multiple layers of pre-tensioned, thin-film membranes that are supported by deployable booms.¹ The behavior of large, thin-film membrane structures needs to be well understood to fully analyze and evaluate observatory dynamics. Models of thin-film membrane structures are difficult to analyze using standard modeling techniques. One problem is that the structure exhibits nonlinear behavior due to the presence of large wrinkles produced by the tensioning forces. Modeling techniques have been developed to take into account the presence of wrinkles, however, these modeling methods have to be validated through comparison with test results.²⁻⁴ Ground testing of large lightweight structures is challenging because (1) they are not designed to support their own weight in a 1-g environment, (2) air has a significant effect on the structural response (e.g. damping, drag, and mass), and (3) traditional instrumentation has a significant influence on membrane behavior. Subscale systems are much less sensitive to gravity and can fit into available vacuum chambers, minimizing the effects of gravity and air. Another issue is manufacturing limitations on film thickness which often cannot be reduced. Constant thickness scaling laws⁵ have been developed to design subscale models by keeping a constant film thickness. These laws allow comparison of the subscale dynamics with the full size system. To mitigate risks associated with sunshield dynamics, a program of analysis and ground testing was undertaken by the government NGST team. The focus of these efforts is a subscale model of the NGST 'yardstick' concept sunshield. Several series of tests have been performed on this model.⁶⁻⁷ This paper describes the results of the last two series of ground tests performed in 2000 and 2001 to characterize the dynamic behavior of the one-tenth-scale model NGST sunshield.

TEST SETUP

The same general setup was used for both test series. It was developed to accept two orientations of the sunshield and to be used in either laboratory (in air) or thermal-vacuum (T/V) chamber environments. The setup is composed of four subsystems: (1) the test article, (2) the test support structure, (3) the excitation system, and (4) the instrumentation.

The test article, Figure 1, consists of a support structure, the membranes, and membrane-support structure interface hardware. The support structure consists of a central block made of aluminum supporting four aluminum tubes in a cruciform manner. The support tubes are circular cross-section tubes with an outside diameter of 0.0159 m (0.625 in.) and a wall thickness of 0.00165 m (0.065 in.). Four membrane layers of 1.27E-05 m thick (0.0005 in), coated Kapton are attached to the central block, two on each side of the structure. Each tube tip has an interface system, Figure 2, composed of a ladder to keep the membrane spacing constant. Constant force springs (CFS) attached to the ladders produce a constant tensioning in the membrane layers. The baseline (CFS1) spring constant of 1.425 N (0.32 lb) was chosen based on the 'yardstick' sunshield design. These baseline springs result in average membrane stresses on the order of 70 kPa (10 psi). During the first test series only the baseline springs, CFS1, were used. During the second test series additional sets of CFS's were tested to characterize the effect of membrane tension on the sunshield dynamics: CFS2 = 2.85 N (0.66 lb) and CFS3 = 4.27 N (0.99 lb).

The test support structure (test stand), Figure 3, is a stiff framework of welded aluminum members composed of the following four sub-assemblies: base plate, column, support legs, and platform. The test stand has a footprint of 1.73 m by 0.76 m (68 in. by 30 in.) with a height of approximately 2 m (78 in.). The column supports the test article at a suitable location, and the support legs provide additional stiffness for the column. The excitation system (shaker) is located on the platform at the top of the column. The test article is mounted in a vertical orientation by fastening the central block directly to the shaker armature. The sunshield can be mounted on the test stand in two configurations: long side down (LSD) and short side down (SSD), Figure 4. The test stand was designed such that its fundamental frequency was above the frequency range of interest for the test article to avoid any coupling.

The test article and stand are instrumented with a series of tri-axial accelerometers and a force transducer. The stand has accelerometers located on the base plate and along the column (Figure 5). The sunshield is instrumented with tri-axial accelerometers located at the tip of each tube and on the central block. The force transducer is located at the interface between the central block and the armature. A non-contact measurement system (laser vibrometer) is used to measure the velocity of the outer layer membrane at different locations. The laser vibrometer is operated in two different modes: (1) as a single point measurement device while the sunshield is subject to random excitation and (2) as a scanning system during sine dwell excitation at specific frequencies (mode shape recovery).

TEST PROCEDURES

A fixture survey was performed once the test stand was installed in the T/V chamber. This was done for both test series and was meant to verify that the fixture modes were sufficiently out of the range of the anticipated sunshield modes. This was a concern because the boundary conditions of the chamber are more compliant than desired. The first fixture modes were approximately 10 Hz bending in Y, and 11 Hz bending in Z and varied slightly between tests. The sunshield was excited in the Z-axis for the tests. Additionally, a mode of the shaker armature suspension was identified at 0.4 Hz. This mode is a rigid body mode of the sunshield moving with the armature in the Z-direction (out-of-plane direction for the sunshield).

During the second test series, a preliminary test was performed with the sunshield support structure mounted on the test stand without the membranes installed. This gave a baseline set of results for the sunshield support structure (tubes) that could be compared to the complete sunshield results to help determine the effect of the membranes on the sunshield dynamics.

Once the sunshield, including the membranes, was installed on the test stand, two types of tests were run under vacuum to characterize the sunshield dynamics: (1) random excitation using the laser vibrometer to measure at fixed locations on the membrane and (2) sine dwell excitation for membrane mode shape recovery.

Random Excitation

Random excitation tests were performed to measure frequency response functions from which the natural frequencies, damping coefficients, and mode shapes for the system can be identified. The tests were completed at an excitation level of 10 mg rms in the Z-direction measured at the central block. The reference channel used to generate FRF's was the single

force transducer located at the interface between the central block and the shaker armature (drive point). Measurements were made at discrete points on the outer layer membrane using the laser vibrometer. During the first test series in 2000 33 points were used. During the second test series in 2001, 22 points were used. Figure 6 shows where the points were located on the membrane for each test series. The change in the number of points was made to shorten data acquisition time and allow more tests to be run in the limited amount of time in the T/V chamber. As a result, not all of the points used for the first test series had a corresponding point for the second test series.

Sine Dwell Excitation

Fine-scale mode shape recovery for the outer membrane layer was accomplished using the laser vibrometer in scanning mode with the test article under constant frequency sine excitation. The frequencies at which the tests were performed were determined from the random excitation test results. The laser vibrometer system has a feature called a "lock-in amplifier" that is used for the sine dwell tests. The lock-in amplifier is essentially a tracking filter that uses a reference signal to determine frequency and then determines the amplitude and phase of the response velocity relative to the reference signal. While using the lock-in amplifier, the laser vibrometer sensor head can be set to scan across the test item using a user-defined number of points. The velocity magnitude and phase information for each point is captured and stored. Post processing of this data provides velocity contours that can be interpreted as mode shapes. The excitation level used for all the sine dwell tests was 15 mg peak (~10 mg rms) and was monitored using the central block accelerometer and an oscilloscope/volt meter. Only the laser vibrometer was used for these tests, no other data was recorded. The number of scan points varied from 550 to 900 points between the test series.

TEST RESULT COMPARISON

Random Excitation Results

There were two test article configurations tested during both the 2000 and the 2001 test series. These were the CFS1, LSD and the CFS1, SSD configurations. It is the results for these configurations that will be compared here. The testing that was performed resulted in a set of measured frequency response functions (FRF's) for each test configuration, consisting of both acceleration and velocity FRF's. Before the analyses could be performed, the velocity FRF's were differentiated and combined with the accelerometer FRF's to form complete sets of acceleration FRF's. Modal parameters were then estimated for each test configuration, see Table 1. In addition to the parameters listed in Table 1, there were also a few modes identified that appear to be local modes of different areas of the membranes. The comparison of the synthesized and measured FRF's was improved at the membrane nodes when these modes were included. The test to test comparison will concentrate on the more global modes. Also note that the modes marked with an [†] are the major system modes involving the interaction of the membranes and the support tubes. The last mode in each list, with a frequency between 10 and 11 Hz, is the first Z bending mode of the test stand. To compare the results, modal assurance criteria (MAC) matrices were calculated. Because the membrane measurement points were not the same between tests, the node locations included in the MAC calculation were chosen based on a geometric correlation. The accelerometer locations were the same between tests so all of those nodes were used. The membrane nodes were first chosen based on a geometric tolerance of 10 cm (4 in.). That is, if the measurement node location from one test was within 10 cm of a node from the other test, it was included in the MAC calculation. Using this tolerance value, 37 out of 49 measurement nodes were used in the MAC calculation. Tables 2 and 3 list the MAC values for the SSD and LSD configurations, respectively. These MAC values do not show very good correlation between the results of the two test series. To see what effect the geometric tolerance might have on the correlation, the geometric tolerance was tightened to 2.5 cm (1 in.) and the MAC's calculated again. The 2.5 cm tolerance resulted in 21 out of 49 measurement nodes being used in the MAC calculation. Tables 4 and 5 list the MAC values for the SSD and LSD configurations, respectively. These MAC values are slightly better but still do not show very good correlation between the results of the two test series. To completely remove the variation in the membrane measurement locations, an analysis was performed using only the degrees of freedom that correspond to accelerometer measurement locations. A subset of the original set of FRF's consisting of only the accelerometer measurements was used to re-estimate the modal parameters. The resulting parameters from this analysis are shown in Table 6. It is a smaller set of parameters than the ones in Table 1 because the low frequency modes that only involve the membrane do not contribute to the response measured at the accelerometer locations. MAC matrices were generated based on this set of results. Since only the accelerometer measurements were used, it was not necessary to do a geometric correlation to compare the results. Tables 7 and 8 list the MAC values for the SSD and LSD configurations, respectively.

These MAC values are much higher (better) than the ones for the results based on the full data set. They show a reasonable correlation between the results of the two test series, with MAC values >0.95 for the medium tube modes and values >0.80 for the long tube modes. It is important to note here that there are pairs of modes that appear to correlate well. One pair, in the 3-4 Hz range, are the out-of-plane modes involving the long tube, while the other pair, in the 5-6 Hz range, are the out-of-plane modes involving the medium tube. It is difficult to distinguish them apart when looking at only the accelerometer data because the difference between the modes primarily involves the membrane and its phasing with the tube.

The results of the two test series show that the sunshield support structure response correlates well from test to test. The membrane response, however, does not correlate as well. The participation of the membranes, especially for the "membrane only" modes, seems to be different from test to test. It is evident, and consistent from test to test, that the presence of the membranes does change the support structure response. Data was collected during the 2001 test series on just the support structure without the membranes installed. The data showed a single fundamental out-of-plane (Z-direction) mode for each support tube. See Table 9 for a summary of the modal parameters for this configuration. The data from both test series has shown that when the membranes are installed, there are generally two out-of-plane modes that involve each support tube. The frequencies of these modes are near the fundamental frequency of the corresponding tube without the membranes installed. Another observation is that the damping is higher with the membranes installed. Figure 7 is a representative set of FRF plots that demonstrates the effect of adding the membranes to the support structure. The data is taken from the 2001 test series with the tubes and sunshield in the SSD configuration. The greatest effect is seen in the plots of the long and medium tube tip locations, which are shown in Figure 7.

Sine Dwell Excitation Results

The velocity contours obtained using the laser vibrometer during sine dwell excitation have been used in a more qualitative than quantitative manner. Modal parameters are not estimated from the data, but because the data is collected at a very large number of points on the membrane, the contours provide a useful qualitative comparison to analytic mode shapes. Even though the modal frequencies vary slightly from test to test as seen in the random test results, the overall mode shapes are fairly similar. This can be seen in the velocity contour plots from the laser vibrometer. Figure 8 shows the contours for one of the modes involving the interaction of the long tube and the membranes for the SSD configuration. The shapes are very similar. Figure 9 shows a similar comparison of contours for one of the modes involving the interaction of the long tube and the membranes for the LSD configuration. Again, the shapes are very similar. The shapes are also similar for the contours of the modes involving the interaction of the medium tube and the membranes. Some differences are seen in the shapes for the modes at the lower frequencies that primarily involve only the membrane. Figure 10 is an example of one of the lower frequency modes for the SSD configuration. The phasing is similar between the shapes but there is a difference in the amplitudes in some areas on the membrane.

CONCLUSION

A significant amount of data has been collected and analyzed for the two test series on the $1/10^{\text{th}}$ scale NGST sunshield. The results of the sunshield support structure correlate reasonably well from test to test. However, the results of the membrane do not correlate well. On a qualitative level, the mode shapes obtained from the sine dwell tests are very similar for modes involving interaction of the support tubes and membranes but exhibit a few differences for modes involving only membrane participation. This is a similar result to the test-analysis correlation that was done for each test.^{3,8-9} The support structure response correlated reasonably well but the membrane response correlation was not as good. One of the other areas of concern with the sunshield is the effect of gravity on the sunshield while testing on the ground. The purpose of testing in both SSD and LSD configurations was to determine that effect. Details of the gravity effect have been presented in previous papers⁶⁻⁷ but examination of Table 1 gives a general indication of the effect. The modal frequencies are slightly different between the SSD and the LSD results and there are fewer modes for the LSD configuration. This is consistent between the two test series.

The one-tenth scale model sunshield studies have resulted in an increase in our capabilities to predict and verify sunshield structural performance that will benefit development of flight sunshield structures. Additionally, these studies are relevant to other gossamer (very large, ultra-lightweight) space structure applications such as solar sails, inflatable antennas, and membrane optics.

REFERENCES

1. Bely, P.Y., Perrygo, C., and Burg, R., NGST "Yardstick" Mission, NGST Monograph No. 1, July 1999.
2. Sebastien Lienard, "Characterization of Large Thin Film Membrane Dynamic Behavior with UAI-NASTRAN Finite Element Solver," October 1999, SAE 1999-01-5518.
3. Johnston, J. and Lienard, S., "Modeling and Analysis of Structural Dynamics for a One-Tenth Scale Model NGST Sunshield," 42nd AIAA Structures, Structural Dynamics, and Materials Conference, Seattle, WA, April 16-19, 2001, AIAA-2001-1407.
4. Adler, A.L., Mikulas, M.M., and Hedgepeth, J.M., "Static and dynamic Analysis of Partially Wrinkled Membrane Structures," 41st AIAA Structures, Structural Dynamics, and Materials Conference, Atlanta, GA, Paper No. AIAA-2000-1810, April 2000.
5. G. Greschik, M. M. Mikulas, and R. E. Freeland, "The Nodal concept of Deployment and the Scale Model Testing of its Application to a Membrane Antenna," April 1999, AIAA 99-1523.
6. Lienard, S., Johnston, J., Ross, B., Smith, J., "Dynamic Testing of a Subscale Sunshield for the Next Generation Space Telescope (NGST)," 42nd AIAA Structures, Structural Dynamics, and Materials Conference, Seattle, WA. Paper No. AIAA-2001-1268, April 2001.
7. Ross, B., Johnston, J., Smith, J., "Parametric Study of the Effect of Membrane Tension on Sunshield Dynamics," 43rd AIAA Structures, Structural Dynamics, and Materials Conference, Denver, CO. Paper No. AIAA-2002-1459, April 2002.
8. Johnston, J. "Finite Element Analysis of Wrinkled Membrane Structures for Sunshield Applications, 43rd AIAA Structures, Structural Dynamics, and Materials Conference, Denver, CO, April 22-25, 2002, AIAA-2002-1456.
9. Johnston, J., Ross, B., Blandino, J., Lawrence, J., and Perrygo, C., "Development of Sunshield Structures for Large Space Telescopes," Proceedings of the 2002 SPIE Astronomical Telescopes and Instrumentation Meeting, Kona, HI, August 24-28, 2002, SPIE paper 4850-24.

Table 1: Summary of modal parameters based on complete data set

(Note: Modes marked with an [†] are the major system modes involving the interaction of the membranes and the support tubes)

Mode #	SSD Configuration				LSD Configuration			
	2000 Test Results		2001 Test Results		2000 Test Results		2001 Test Results	
	f (Hz)	ξ (%)	f (Hz)	ξ (%)	f (Hz)	ξ (%)	f (Hz)	ξ (%)
1	1.58	8.09	1.49	5.77	1.46	5.60	1.32	7.29
2	1.78	7.09	1.89	6.37	2.32	6.90	1.42	5.97
3	1.84	6.17	2.07	6.29	2.71	6.20	2.70	5.75
4	2.36	8.00	3.02 [†]	6.69	3.40 [†]	2.90	3.35 [†]	3.18
5	2.99 [†]	4.71	3.21 [†]	3.67	4.50 [†]	3.10	4.15	4.26
6	3.48 [†]	4.86	3.84	4.99	5.48 [†]	2.50	4.42	8.17
7	4.12	5.55	4.79	5.23	10.54	0.50	5.51 [†]	2.57
8	4.87	5.28	4.85	5.39			10.87	0.24
9	5.09 [†]	5.61	5.83 [†]	4.96				
10	5.96 [†]	3.27	10.84	0.33				
11	10.54	0.53						

Table 2: MAC matrix for SSD, complete dataset, geometric tolerance for membrane points = 10 cm

		2000 Test Identified Modes (Hz)										
		1.58	1.78	1.84	2.36	2.99	3.48	4.12	4.87	5.09	5.96	10.54
2001 Test Identified Modes (Hz)	1.49	0.62	0.00	0.01	0.02	0.00	0.00	0.02	0.01	0.01	0.02	0.03
	1.89	0.01	0.67	0.12	0.49	0.00	0.02	0.01	0.00	0.01	0.00	0.00
	2.07	0.00	0.00	0.39	0.03	0.19	0.01	0.02	0.00	0.00	0.00	0.02
	3.02	0.07	0.00	0.00	0.11	0.15	0.51	0.25	0.00	0.00	0.00	0.01
	3.21	0.00	0.00	0.05	0.12	0.22	0.18	0.23	0.03	0.01	0.00	0.01
	3.84	0.00	0.00	0.04	0.02	0.01	0.02	0.06	0.10	0.05	0.01	0.09
	4.79	0.00	0.01	0.01	0.00	0.00	0.08	0.02	0.21	0.21	0.03	0.07
	4.85	0.01	0.02	0.01	0.00	0.00	0.07	0.04	0.05	0.27	0.00	0.08
	5.83	0.04	0.01	0.04	0.00	0.02	0.02	0.00	0.05	0.00	0.40	0.06
	10.84	0.00	0.01	0.00	0.12	0.00	0.03	0.12	0.00	0.00	0.02	0.00

Table 3: MAC matrix for LSD, complete dataset, geometric tolerance for membrane points = 10 cm

		2000 Test Identified Modes (Hz)						
		1.46	2.32	2.71	3.40	4.50	5.48	10.54
2001 Test Identified Modes (Hz)	1.32	0.21	0.04	0.03	0.00	0.00	0.00	0.02
	1.42	0.50	0.19	0.12	0.03	0.01	0.00	0.00
	2.70	0.16	0.12	0.15	0.05	0.00	0.00	0.27
	3.35	0.04	0.05	0.04	0.11	0.02	0.00	0.02
	4.15	0.00	0.00	0.02	0.00	0.16	0.00	0.00
	4.42	0.00	0.05	0.04	0.02	0.36	0.04	0.00
	5.51	0.00	0.01	0.04	0.01	0.13	0.36	0.06
	10.87	0.01	0.00	0.01	0.02	0.02	0.01	0.04

Table 4: MAC matrix for SSD, complete dataset, geometric tolerance for membrane points = 2.5 cm

		2000 Test Identified Modes (Hz)										
		1.58	1.78	1.84	2.36	2.99	3.48	4.12	4.87	5.09	5.96	10.54
2001 Test Identified Modes (Hz)	1.49	0.56	0.08	0.16	0.00	0.10	0.02	0.00	0.36	0.87	0.03	0.13
	1.89	0.10	0.00	0.01	0.56	0.46	0.52	0.15	0.22	0.04	0.00	0.01
	2.07	0.00	0.00	0.00	0.77	0.83	0.56	0.41	0.00	0.01	0.01	0.00
	3.02	0.09	0.02	0.00	0.82	0.67	0.89	0.55	0.03	0.02	0.01	0.00
	3.21	0.01	0.02	0.01	0.88	0.91	0.70	0.51	0.00	0.01	0.00	0.01
	3.84	0.19	0.03	0.02	0.13	0.27	0.19	0.20	0.16	0.05	0.02	0.00
	4.79	0.72	0.50	0.38	0.07	0.00	0.20	0.06	0.21	0.08	0.05	0.25
	4.85	0.75	0.47	0.35	0.05	0.01	0.13	0.25	0.00	0.14	0.04	0.15
	5.83	0.01	0.05	0.05	0.02	0.02	0.04	0.00	0.21	0.02	0.77	0.30
	10.84	0.14	0.00	0.00	0.00	0.01	0.00	0.00	0.07	0.08	0.01	0.00

Table 5: MAC matrix for LSD, complete dataset, geometric tolerance for membrane points = 2.5 cm

		2000 Test Identified Modes (Hz)						
		1.46	2.32	2.71	3.40	4.50	5.48	10.54
2001 Test Identified Modes (Hz)	1.32	0.29	0.00	0.24	0.13	0.00	0.25	0.00
	1.42	0.31	0.04	0.02	0.02	0.46	0.03	0.00
	2.7	0.05	0.15	0.03	0.02	0.01	0.01	0.04
	3.35	0.05	0.09	0.18	0.31	0.08	0.01	0.05
	3.76	0.01	0.36	0.19	0.19	0.14	0.00	0.04
	4.15	0.06	0.05	0.03	0.03	0.49	0.01	0.02
	4.42	0.06	0.01	0.02	0.04	0.63	0.05	0.05
	5.51	0.02	0.27	0.08	0.00	0.14	0.37	0.12
	10.87	0.15	0.13	0.02	0.01	0.06	0.08	0.04

Table 6: Summary of modal parameters based on accelerometer data only

Mode #	SSD Configuration				LSD Configuration			
	2000 Test Results		2001 Test Results		2000 Test Results		2001 Test Results	
	f (Hz)	ξ (%)	f (Hz)	ξ (%)	f (Hz)	ξ (%)	f (Hz)	ξ (%)
1	2.99	6.32	3.20	4.09	3.43	2.80	3.34	3.04
2	3.50	6.50	3.88	4.64	4.10	2.80	4.11	3.27
3	4.08	6.00	4.83	5.45	4.52	3.20	5.51	2.52
4	4.98	5.50	5.86	5.39	5.50	2.50	10.87	0.26
5	5.98	3.85	10.86	0.25	10.54	0.50		
6	10.54	0.51						

Table 7: MAC matrix for SSD configuration, accelerometer data only

		2000 Test Identified Modes (Hz)					
		2.99	3.5	4.08	4.98	5.98	10.54
2001 Test Identified Modes (Hz)	3.20	0.89	0.82	0.80	0.00	0.04	0.07
	3.88	0.80	0.78	0.60	0.03	0.08	0.06
	4.83	0.00	0.01	0.03	0.96	0.99	0.07
	5.86	0.00	0.00	0.02	0.95	0.99	0.08
	10.86	0.05	0.04	0.03	0.04	0.06	0.61

Table 8: MAC matrix for LSD configuration, accelerometer data only

		2000 Test Identified Modes (Hz)				
		3.43	4.10	4.52	5.50	10.54
2001 Test Identified Modes (Hz)	3.34	0.99	0.49	0.00	0.02	0.07
	4.11	0.60	0.74	0.09	0.03	0.02
	5.51	0.02	0.01	0.98	1.00	0.07
	10.87	0.04	0.00	0.07	0.08	0.82

Table 9: Summary of modal parameters for support structure without membranes (tubes only)

Mode #	SSD Configuration		LSD Configuration	
	f (Hz)	ξ (%)	f (Hz)	ξ (%)
1	3.43	0.30	3.63	0.32
2	5.92	0.71	5.75	0.15
3	11.03	0.54	10.97	0.53

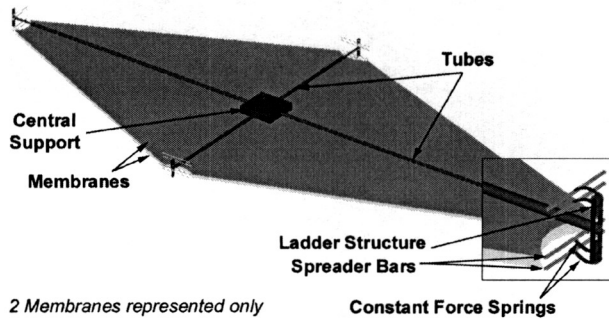


Figure 1: 1/10th scale NGST sunshield test article

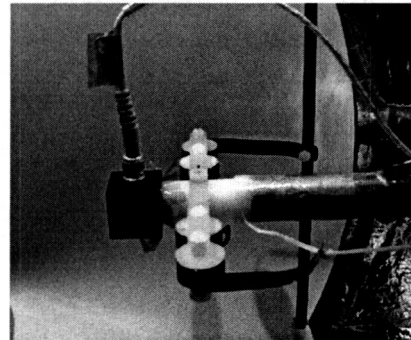


Figure 2: Tip ladder structure and CFS

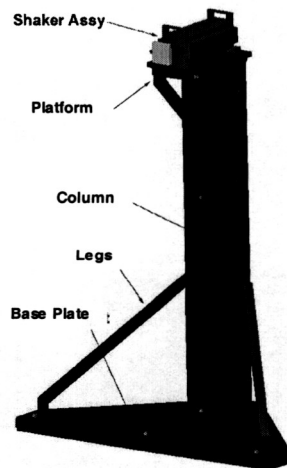


Figure 3: Subscale sunshield test stand

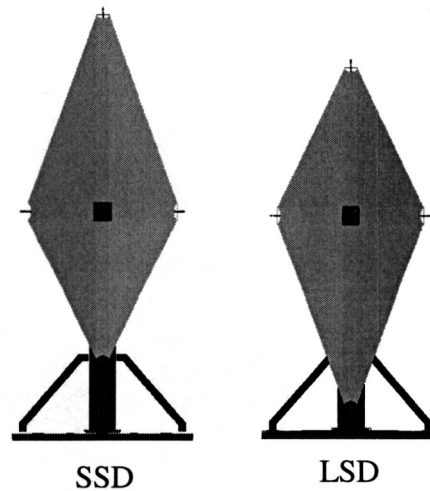


Figure 4: Sunshield test configurations

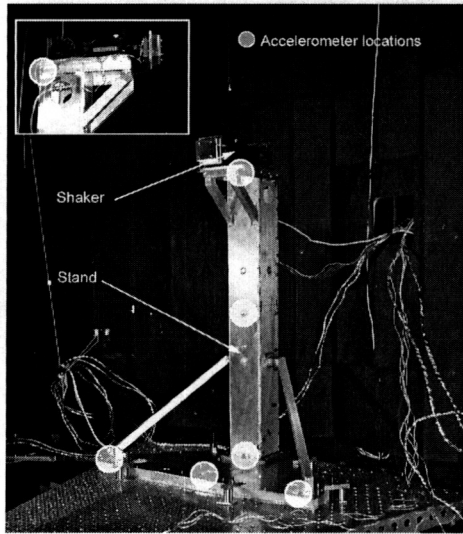


Figure 5: Accelerometer locations on test stand

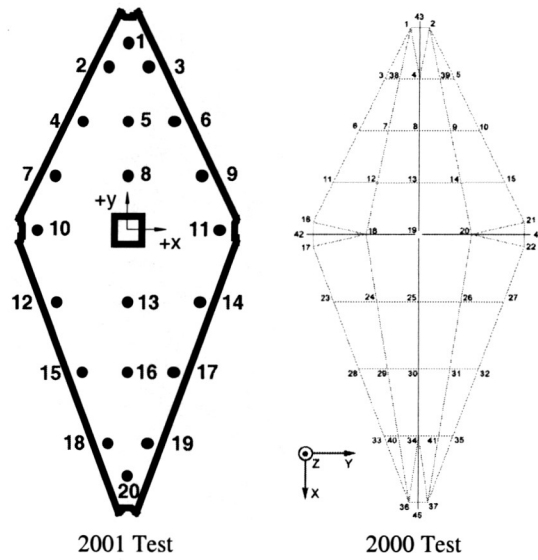


Figure 6: Membrane measurement locations

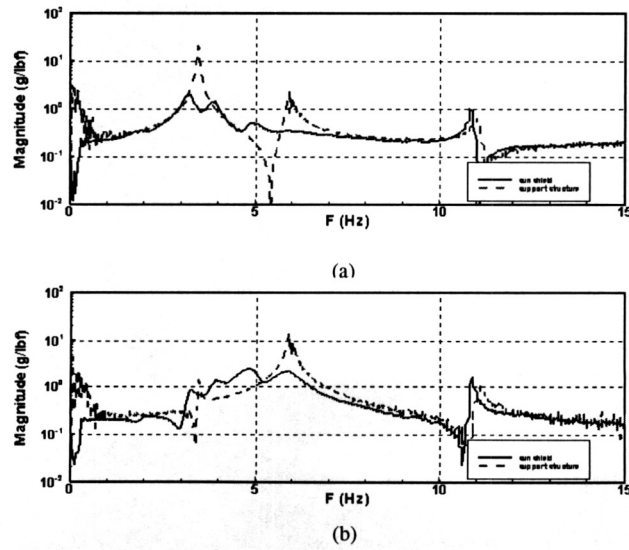


Figure 7: Tube response, with and without membranes for long tube (a) and medium tube (b)

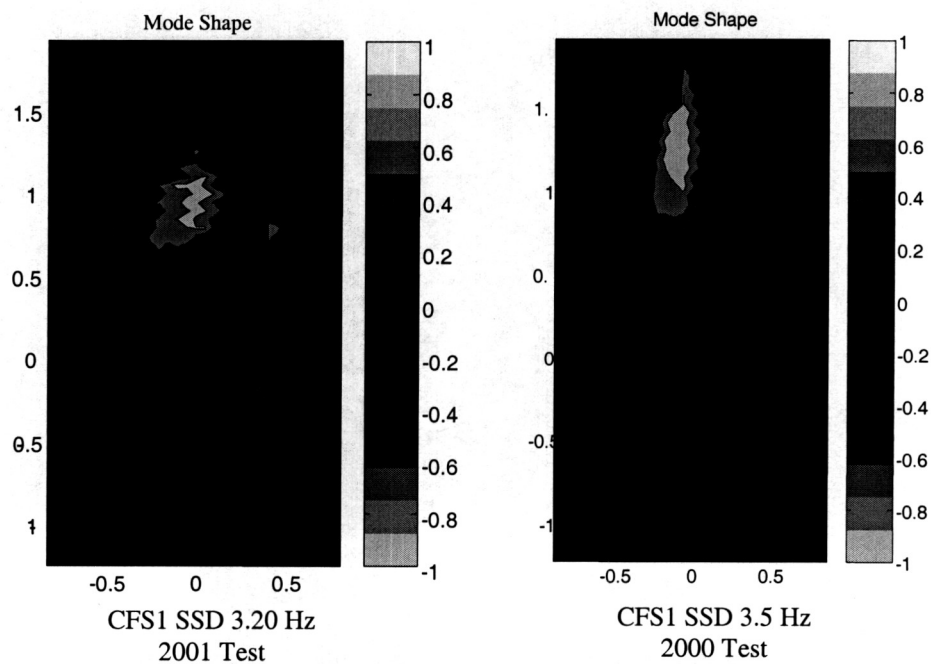


Figure 8: Velocity contour (mode shape) comparison for mode involving long tube in SSD configuration

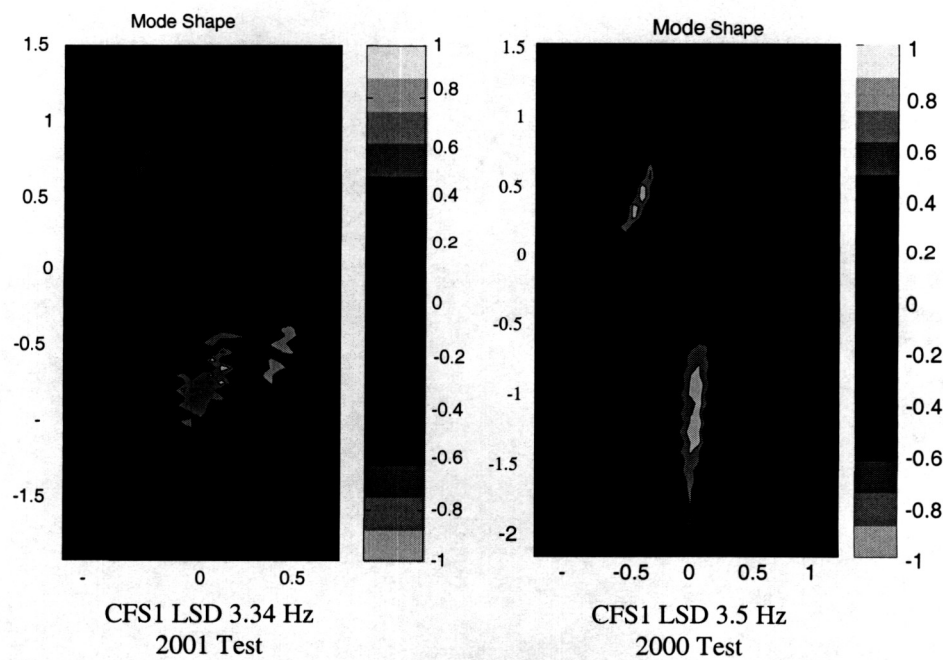


Figure 9: Velocity contour (mode shape) comparison for mode involving long tube in LSD configuration

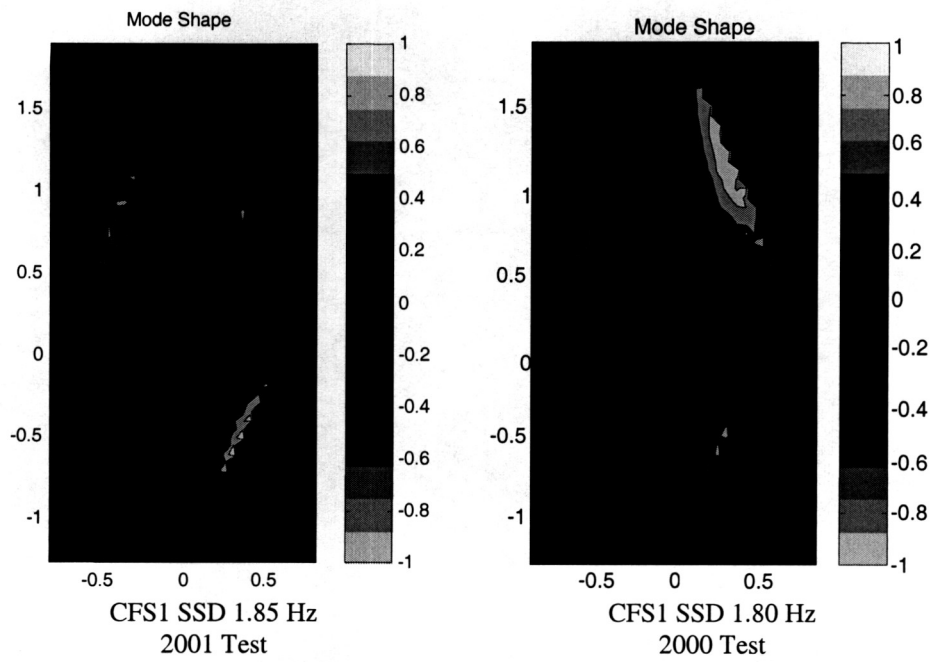


Figure 10: Velocity contour (mode shape) comparison for membrane mode in SSD configuration